CORRELATION OF COMPOSITIONAL PHASES AND WETTABILITY-BASED FLUID-TRACERS IN FINE-GRAINED RESERVOIRS

Qinhong Hu[1]; Jamil J. Clarke[2]; Rod Baird[2]; Chad Ostrander[2]; Zhiye Gao[3]; Yuxiang Zhang[1]; Kibria Golam[1]
[1]The University of Texas at Arlington, Arlington, TX 76019, USA.
[2]Hitachi High Technologies America, Inc., Clarksburg, MD 20871, USA.
[3]State Key Laboratory of Petroleum Resources and Prospecting, China University of Petroleum, Beijing 102249, China.

This paper was prepared for presentation at the International Symposium of the Society of Core Analysts held in St. John's, Newfoundland and Labrador, Canada, 16-21 August, 2015

ABSTRACT

Fine-grained reservoirs can contain distinct compositional phases, with oil-wetting organic matter/carbonate and other water-wetting mineral phases. Despite their importance in hydrocarbon storage and production, the intertwined wettability, nanopore distribution, and pore connectivity of these phases are not well understood. The approach presented here involves tracers in two fluids (API brine and *n*-decane) that are used to specifically interrogate the spatial wettability of organic-matter and mineral phases, through an integrated approach of phase imaging by Scanning Electron Microscopy (SEM) and tracer mapping with laser ablation-inductively coupled plasma-mass spectrometry (LA-ICP-MS). A core sample from Eagle Ford was used for a testing area of 2.1mm×1.8mm that was argon-ion milled and imaged with a Hitachi SU3500 SEM with image montage (Zig-Zag) capabilities for compositional distribution. The same sample area was then treated with tracers in brine and *n*-decane fluids, followed with LA-ICP-MS mapping for tracer distribution at different spatial resolutions (8μm, 12μm, and 75μm). A negative correlation between brine-tracers (ReO_4^- and Eu^{3+}) and *n*-decane-tracer of 1-iododecane was observed.

INTRODUCTION

Since 2000, the technological advances of horizontal drilling and hydraulic fracturing in North America have led to a dramatic increase in hydrocarbon (gas and oil) production from shale formations, changing the energy landscape in the U.S.A. and worldwide. However, the sustainable shale resource development is implicated by the steep hydrocarbon production decline and overall low recovery. For example, the top five US resource plays typically produced 80–95% less gas after 3 years, and the productivity of new wells in two leading tight-oil plays (Bakken and Eagle Ford) dropped by about 60% within the first year [1]. Total gas recovery from the Barnett, the most developed shale play, was reported to be only 8–15% of gas-in-place in 2002, and 12–30% in 2012 [2]. The recovery rate for tight oil is even lower at 5–10% [3].

Hydrocarbon storage and production in hydraulically-stimulated shale are affected by the intertwined correlation of compositional phases, wettability, nanopore distribution, and pore connectivity of shales. As shales contain distinct oil-wetting organic-matter (e.g., kerogen) and water-wetting mineral phases, the novel method of unique tracers in two fluids to interrogate the wettability and connectivity of organic-matter and mineral pore spaces is realized in this work. The organic fluid (*n*-decane) is expected to be preferentially attracted to the hydrophobic component (e.g. organic particle) of the shale matrix, with reported sizes ranging from less than 1μm to tens of μm [4]. Organic grains are found to be dispersed through the matrix of shales such as Barnett [2], but their connection through surrounding mineral phases is unknown, despite its implication in steep initial decline and low overall recovery.

This paper presents our collaborative studies of correlating compositional phases from SEM imaging (performed at Hitachi High Technologies America of Clarksburg, MD) with wettability-tracers and laser ablation-ICP-MS (LA-ICP-MS) elemental mapping at the University of Texas at Arlington.

PROCEDURES

In this work, we used a proprietary core sample from Eagle Ford to develop the technical approaches and showcase the findings. The sample was cut into a rectangular bar with a width and length of ~2.2 mm and height of ~10 mm. The sample surface was first milled with a Hitachi Ar-ion milling system (Model IM4000, Hitachi High Technologies America, Inc.). At a maximum milling rate of 300 μm/h for silicon, this broad ion milling system was used to prepare a high-quality cross-section. An area of 4.867mm^2 was processed by two 4-hr mill sessions at a voltage acceleration energy of 6 kV with a stage swing of ±40° (Fig. 1A). The area of 2,147μm×1,799μm (the shaded region of Fig. 1B) was then used for producing an image montage by Zig-Zag function of a Hitachi SU3500 SEM. The SU3500 SEM has a variable-pressure design that eliminates the need for coating non-conductive materials for image acquisition. An acceleration energy of 5kV was applied to the SEM for acquiring images at a magnification of 1,000 times. Each image was captured at a resolution of 2,560×1,920, with 8-bit grayscale, 512×512 dpi, and 121.3 μm horizontal field width (Fig. 1C). The image montage was composed of 460 images that were stitched together, and the total time to acquire the entire image tile array was ~7 hrs with the integrated Zig-Zag function which automates the entire process. The image tiles were acquired along with a 20% margin of overlap, and this margin is needed for the stitching software to align each image tile on all four sides. In addition, this margin also includes some mechanical stage movement backlash which is why the margin percent is needed to compensate for this deficit. Therefore, each image tile is not a true side by side acquisition but a series of semi-overlapping images.

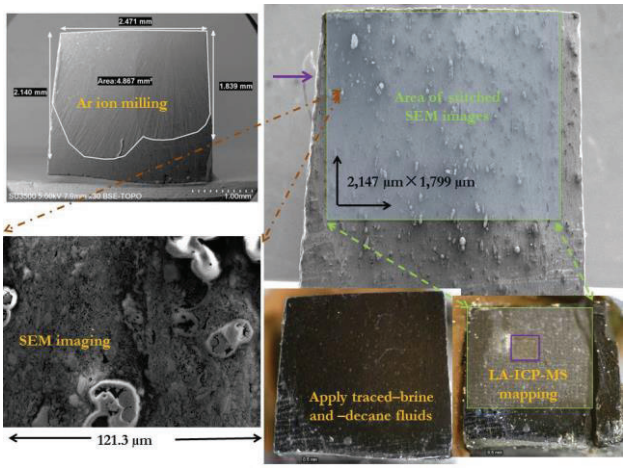

Figure 1. Work flow of Ar ion milling, SEM imaging, and elemental mapping of applied wettability-tracers (scale bars are shown for each graph).

We used 0.1 mM each of $NaReO_4$ and $EuBr_3 \cdot 6H_2O$ (Sigma-Aldrich Co., St. Louis, MO) dissolved in API brine (8% NaCl and 2% $CaCl_2$ by weight, with perrhenate anion (ReO_4^-) and europium cation (Eu^{3+}) as non-sorbing and sorbing tracers, respectively. For organic-phase *n*-decane tracer, organic-I (1-iododecane) [$CH_3(CH_2)_9I$, molecular weight of 268.18 g/mol] (>99% pure, Sigma-Aldrich Co.] was directly added to *n*-decane fluid at a volume ratio of 1%. The elements rhenium (Re), europium (Eu), and iodine (I) of these tracer chemicals are readily detected by LA–ICP–MS.

To investigate the association of wettability to compositional phases, we applied one drop (0.16 mL) of brine tracer solution in the middle of an imaged area, and waited for an hour for the beaded-up fluid to slowly evaporate and spread on and within the sample. Next, an additional drop of brine tracer (Fig. 2A-B) was applied. After another hour, some localized zones of salt precipitates were observed and removed with a razor blade (Fig. 2C-D). Two drops of *n*-decane tracers were then applied, in a similar fashion as brine at two settings; *n*-decane was found to quickly spread on the sample surface (Figure not shown), which was much different from API brine. After seven hours that the 1st application of brine tracer was dropped, LA–ICP–MS mapping analyses were performed on the sample (Fig. 1D).

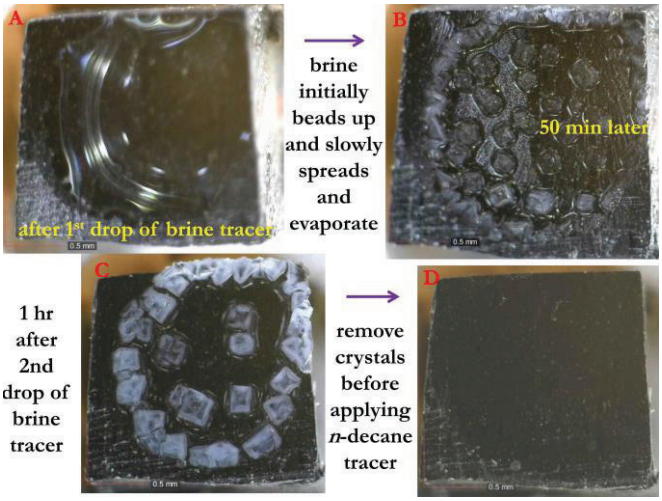

Figure 2. Spreading behavior of traced-API brine on an Eagle Ford sample (a scale bar is shown on each picture).

The laser ablation system (UP-213, New Wave; Freemont, CA) used a 213 nm laser to vaporize a hole in the rock sample at sub-micron depth for each laser pulse; elements entrained in the vapor were analyzed with ICP-MS (PerkinElmer/SCIEX ELAN DRC II; Sheldon, CT). For different research purposes, this LA-ICP-MS approach can generate 2-D and 3-D maps of chemical distributions in rock at a spatial resolution of microns, and a concentration limit of low-mg/kg [5]. For this work, two mapping-area approaches were used. The first, and a wider, mapping area (2,175μm×1,800μm; called Grid A) nearly matched the SEM-imaged area (2,147μm×1,799μm), and we used 75μm as the laser spot size and spacing between spots; the laser was fired for 60 pulses at each spot (Fig. 1D). This produced a total of 750 data spots, a duration of 10 hours for completion. The 2nd, and a finer, grid (Grid B) was located near the middle of the mapped SEM region, and was selected at 500μm below, and to the right of, the starting point of Grid A (Fig. 1D). This finer grid covered an area of 612μm×240μm, and used smaller spot sizes and larger laser pulses (8μm and 400 pulses; 12μm and 200 pulses) in order to collect more sample mass for ICP-MS detection; a total of 26 hrs was taken to complete the mapping of Grid B. During the data processing, the differences in spot size and laser pulse were corrected.

RESULTS

LA-ICP-MS elemental mapping results for Grids A and B are shown as Figs. 3-4. For these figures, the scale bars indicate the measured elemental background level of the analyte in the sample (as the lowest value, and cold color, in scale bar) and detected high concentrations of tracer element (as the highest value, and warm color, in scale bar). Therefore, any color difference in these figures indicates the presence of tracers.

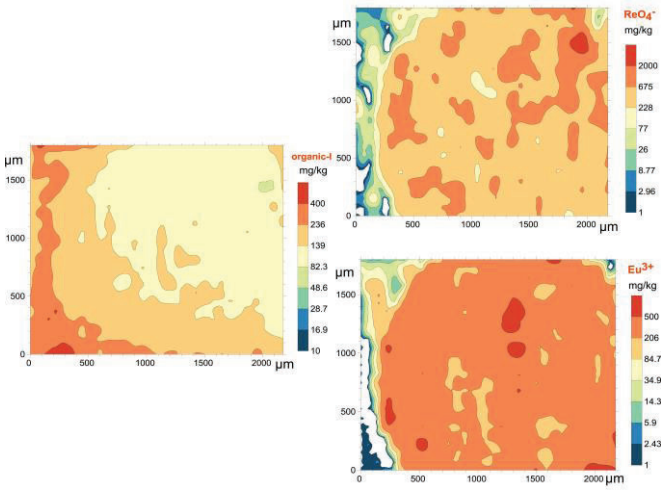

Figure 3. Tracer distribution in Grid A.

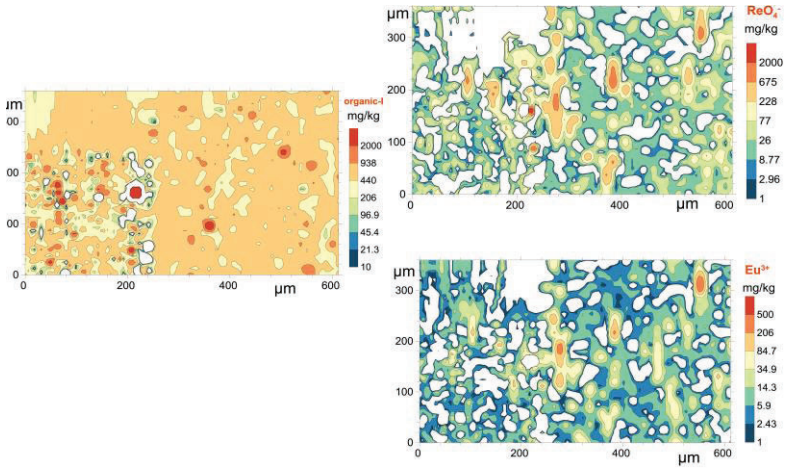

Figure 4. Tracer distribution in Grid B with higher mapping resolutions; the 1st 240 μm (from the left) and 2nd 360 μm zones were mapped at 8 μm and 12 μm spatial resolutions, respectively.

DISCUSSION

The Eagle Ford sample has a high carbonate content [6], which was confirmed from the SEM images showing an abundant presence of coccospheres (Fig. 1C). Carbonate rock tends to exhibit an oil-wetting characteristics[7], consistent with our observed spreading behavior of API brine and *n*-decane. The application of wettability-based tracers and resultant LA-ICP-MS mapping further illustrate the spatial variability of wettability regions, on the scale of microns. Fig. 3 was mapped at the scale of 75 μm and shows relatively less spotty behavior of high-concentration tracer regions than Fig. 4 at finer (8 and 12 μm mapping resolutions). Furthermore, for both Figs. 3-4, brine tracers of ReO_4^- and Eu^{3+} follow the similar pattern, while *n*-decane tracer of organic 1-iododecane shows higher concentrations at different regions from brine tracers. The overall results illustrate the presence of spatially variable water-wetting mineral phases and oil-wetting phase (carbonate for this Eagle Ford sample), which is consistent with other tests (imbibition,

diffusion, and vacuum-saturation for edge-accessible pore spaces) of the sample (results not shown).

CONCLUSIONS

Using an integrated approach of SEM phase imaging and wettability-based tracer mapping of LA-ICP-MS, we illustrate the seemingly negative correlation of API brine-based tracers with *n*-decane tracer to indicate the spatial variability, at microns scale, of water- and oil-wetting compositional phases of an Eagle Ford sample. Using these developed approaches, additional tests will be conducted for shale samples with a range of total organic content to interrogate the wettability patterns, and associated pore sizes, of compositional phases of shale. The integrated studies on intertwined correlation of compositional phases, wettability, nanopore distribution, and connectivity of fine-grained reservoirs will help understand the hydrocarbon storage and production in stimulated reservoirs.

ACKNOWLEDGEMENTS

Funding for this project was partially provided by the Foundation of State Key Laboratory of Petroleum Resources and Prospecting, China University of Petroleum, Beijing.

REFERENCES

1. Hughes, J.D. 2013. *Drill, Baby, Drill: Can Unconventional Fuels Usher in a New Era of Energy Abundance?* Post Carbon Institute, 2013, 178 pp.
2. Hu, Q.H., and R.P. Ewing. *Integrated Experimental and Modeling Approaches to Studying the Fracture-Matrix Interaction in Gas Recovery from Barnett Shale*. Final Report, Research Partnership to Secure Energy for America (RPSEA), National Energy Technology Laboratory, Department of Energy, 2014, 80 pp.
3. Hoffman, T. *Comparison of various gases for enhanced oil recovery from shale oil reservoirs*. This paper was presented for presentation at the Eighteenth SPE Improved Oil Recovery Symposium held in Tulsa, OK, USA, 14-18 April 2012, SPE 154329.
4. Loucks, R.G., R.M. Reed, S.C. Ruppel and D.M. Jarvie. 2009. Morphology, genesis, and distribution of nanometer-scale pores in siliceous mudstones of the Mississippian Barnett Shale. *J. Sed. Res.*, 2009, 79(11-12), 848-861.
5. Hu, Q.H., T.J. Kneafsey, J.S.Y. Wang, L. Tomutsa, and J.J. Roberts. 2004. Characterizing unsaturated diffusion in porous tuff gravels. *Vadose Zone J.*, 2004, 3(4), 1425-1438.
6. Slatt, R.M., N.R. O'Brien, A. Miceli Romero, H.H. Rodriguez. *Eagle Ford condensed section and its oil and gas storage and flow potential*. AAPG Annual Convention and Exhibition, Long Beach, California, April 22-25, 2012. Search and Discovery Article #80245, 2012.
7. Roychaudhuri, B., T.T. Tsotsis, and K. Jessen. An experimental investigation of spontaneous imbibition in gas shales. *J. Petro. Sci. and Eng.*, 2013, 111, 87-97.